

A realistic study of the nuclear transparency  
 and the distorted momentum distributions  
 in the semi-inclusive process  $^4\text{He}(e;e^0p)X$

H. Morita and C. Ciodegliatti

Department of Physics, University of Perugia, and Istituto Nazionale di Fisica Nucleare, Sezione di Perugia, Via A. Pascoli, I-06100 Perugia, Italy

D. Treleani

Department of Theoretical Physics, University of Trieste, Strada Costiera 11, Istituto Nazionale di Fisica Nucleare, Sezione di Trieste, and ICTP, I-34014, Trieste, Italy

(February 21, 2019)

## Abstract

The nuclear transparency and the distorted momentum distributions of  $^4\text{He}$  in the semi-inclusive process  $^4\text{He}(e;e^0p)X$  are calculated within the Glauber multiple scattering approach using for the first time realistic four-body variational wave functions embodying central and non-central nucleon-nucleon (N-N) correlations. The contributions from N-N correlations and from Glauber multiple scattering are taken into account exactly to all orders. It is shown that non-central correlations significantly affect both the transparency and the distorted momentum distributions; as a matter of fact: i) the small ( 3% ) value of the effect of correlations on the transparency results from an appreciable cancellation between the short-range central repulsive correlations and the intermediate-range attractive correlations, whose magnitude is significantly affected by the non-central forces, and ii) the effect of Glauber final state interactions on the momentum distribution is strongly reduced by the inclusion of tensor correlations. Our results are at variance with the ones based on Jastrow wave functions embodying only phenomenological central correlations.

25.30.Fj, 25.10.+s, 24.10. i

Typeset using REVTeX

---

On leave of absence from Sapporo Gakuin University, Bunkyo-dai 11, Ebetsu 069, Hokkaido, Japan

## I. INTRODUCTION

The role played by ground state nucleon{nucleon (NN) correlations on the nuclear transparency in semi-inclusive processes have been investigated by many authors. (see e.g. [1]-[8]) with conflicting results. All of these works adopt the Glauber multiple scattering approach for the description of the final state interaction (FSI), and treat N+N correlations within different schemes and approximations, ranging from phenomenological Jastrow wave functions embodying only central correlations [1], [6] to various expansions in terms of correlated density matrices [2], [3], [4]. Recently, Seki et al. [5] have performed an elaborated calculation of the transparency using, by means of a local density approximation (LDA), realistic nuclear matter correlation functions for finite nuclei, and taking into account Glauber multiple scattering to all orders. Such a calculation represents a significant progress in the field, but it should be pointed out that a direct calculation of the transparency using realistic wave functions resulting from the solution of the many-body problem and implemented by Glauber multiple scattering operators, is still lacking. It is the purpose of this paper to present such a calculation for the  ${}^4\text{He}$  nucleus. We have calculated both the nuclear transparency and the distorted momentum distributions in the process  ${}^4\text{He}(e;e'p)X$ ; the calculation of the distorted momentum distributions represents, to our knowledge, the first realistic calculation of this quantity. As a matter of fact, the distorted momentum distributions have been calculated in a series of recent papers [6], [7], where it has been argued that the high momentum part of the distorted momentum distributions which could be measured by semi-inclusive processes  $A(e;e'N)X$ , are almost entirely dominated by FSI, leaving little room for the investigation of N+N correlations. Unfortunately, those works (except for the deuteron's study) are based on the use of phenomenological Jastrow wave functions constructed from harmonic oscillator orbitals and oversimplified central correlation functions. It will be shown in this paper that the effect of FSI on the momentum distribution obtained from realistic many-body wave functions embodying central and non-central correlations is much smaller than the one found in [6].

Our paper is organised as follows: in Section II the concepts of semi-inclusive processes, distorted momentum distributions and nuclear transparency, will be recalled; the structure of the  ${}^4\text{He}$  wave function used in the calculations will be briefly described in Section III; the results of calculations of the nuclear transparency and the distorted momentum distributions will be presented in Sections IV and V, respectively; the Summary and Conclusions are given in Section VI.

## II. THE CROSS SECTION FOR THE SEMI-INCLUSIVE $A(e;e'p)X$ PROCESS, THE DISTORTED MOMENTUM DISTRIBUTIONS AND THE NUCLEAR TRANSPARENCY

We will consider the process  $A(e;e'p)X$  in which an electron with 4-momentum  $k_1 = \mathbf{k}_1; i_1 g$ , is scattered off a nucleus with 4-momentum  $P_A = \mathbf{P}_A; iM_A g$  to a state  $k_2 = \mathbf{k}_2; i_2 g$  and is detected in coincidence with a proton  $p$  with 4-momentum  $k_p = \mathbf{k}_p; iE_p g$ ; the final ( $A-1$ ) nuclear system with 4-momentum  $P_X = \mathbf{P}_X; iE_X g$  is undetected. The cross section describing the process can be written as follows

$$\frac{d}{dQ^2 d dk_p} = K_{ep} P_D(E_m; k_m) \quad (1)$$

where  $K$  is a kinematical factor,  $\sigma_{ep}$  the on-shell electron-nucleon cross section, and  $Q^2 = \mathbf{q}^2$  the four momentum transfer. The quantity  $P_D(E_m; k_m)$  is the distorted nucleon spectral function which depends upon the observable missing momentum

$$k_m = q - k_p \quad (2)$$

and missing energy

$$E_m = + M - E_p: \quad (3)$$

The latter equation results from energy conservation

$$+ M_A = E_p + \frac{q}{M_X^2 + p_X^2} \quad (4)$$

if the total energy of the system  $X$  is approximated by its non-relativistic expression and the recoil energy is disregarded. The distorted spectral function can be written in the following short-hand form [1]

$$P_D(E_m; k_m) = \int_{f_X}^X j(k_m; f_X) j_A i(f(E_m - E_{m \text{ in}} - E_{f_X})) \quad (5)$$

where  $E_{m \text{ in}} = M + M_{A-1} - M_A$ , and

$$j(k_m; f_X) i = e^{ik_m \cdot r_A} S_G^Y(r_1 :: r_A) \int_{f_X}^X (r_1 :: r_{A-1})_A (r_1 :: r_A) \left( \prod_{j=1}^{A-1} r_j \right) \prod_{i=1}^Y dr_i; \quad (6)$$

with  $j_A$  and  $f_X$  being the ground state wave function of the target nucleus and the wave function of the system  $X$  in the state  $f_X$ , respectively; the quantity  $S_G$  is the Glauber operator, which describes the FSI of the struck proton with the  $(A-1)$  system, i.e.

$$S_G(r_1 :: r_A) = \prod_{j=1}^{A-1} G(r_A; r_j) \prod_{j=1}^{A-1} \left[ \delta(z_j - z_A) \delta(b_A - b_j) \right] \quad (7)$$

where  $b_j$  and  $z_j$  are the transverse and the longitudinal components of the nucleon coordinate  $r_j$  ( $b_j; z_j$ ),  $G$  is the Glauber profile function for elastic proton nucleon scattering, and the function  $\delta(z_j - z_A)$  takes care of the fact that the struck proton "A" propagates along a straight-path trajectory so that it interacts with nucleon "j" only if  $z_j > z_A$ . The integral over the missing energy of the distorted spectral function defines the distorted momentum distribution as

$$n_D(k_m) = \int_{E_m}^Z dE_m P_D(E_m; k_m): \quad (8)$$

In impulse approximation (IA) (i.e. when the final state interaction is disregarded ( $S_G = 1$ )), if the system  $X$  is assumed to be a  $(A-1)$  nucleus in the discrete or continuum states  $f_X = f_{A-1}$ , the distorted spectral function  $P_D$  reduces to the usual spectral function i.e.

$$P_D = \int_{f_{A-1}}^X dk; \quad f_{A-1} \leq k \leq (E_{\text{miss}} + E_{f_{A-1}})) \quad (9)$$

where  $E$  is the nucleon removal energy i.e. the energy required to remove a nucleon from the target, leaving the  $A-1$  nucleus with excitation energy  $E_{f_{A-1}}$  and  $k = k_m = (q - k_p)$  is the nucleon momentum before interaction. The integral of the spectral function over the  $E$  defines the (undistorted) momentum distributions

$$n(k) = \int_0^Z dE P(E; k); \quad (10)$$

In this paper we will consider the effect of the FSI ( $S_G \neq 1$ ) on the semi-inclusive  $A(e; e^0 p)X$  process, i.e. the cross section (1) integrated over the missing energy  $E_m$ , at fixed value of  $k_m$ . Owing to

$$\int_{f_X}^X \frac{(r_1^0 \dots r_{A-1}^0)}{(r_1 \dots r_{A-1})} = \sum_{j=1}^{A-1} \frac{(r_j \quad r_j^0)}{(r_j \quad r_j^0)} \quad (11)$$

the cross section (1) becomes directly proportional to the distorted momentum distributions (8), i.e.

$$n_D(k_m) = (2\pi)^3 \int_0^Z e^{ik_m \cdot (r - r^0)} D(r; r^0) dr dr^0 \quad (12)$$

where

$$D(r; r^0) = \frac{h_A S_G^Y \hat{O}(r; r^0) S_G^0 \frac{0}{A} i}{h_A \frac{0}{A} i} \quad (13)$$

is the one-body fixed density matrix, and

$$\hat{O}(r; r^0) = \sum_{i=1}^X (r_i \quad r) (r_i^0 \quad r^0) \sum_{j \neq i}^Y (r_j \quad r_j^0) \quad (14)$$

the one-body density operator. In Eq. (13) and in the rest of the paper, the primed quantities have to be evaluated at  $r^0$ . By integrating  $n_D(k_m)$  one obtains the nuclear transparency  $T$ , which is defined as follows

$$T = \int_0^Z n_D(k_m) dk_m = (2\pi)^3 \int_0^Z D(r; r^0) dr dr^0 \int_0^Z e^{ik_m \cdot (r - r^0)} dk_m = \int_0^Z D(r) dr \quad (15)$$

i.e.

$$T = \int_0^Z D(r) dr = 1 + T \quad (16)$$

where  $T$  originates from FSI.

We specialize now to the four-body system, for which the use of intrinsic coordinates is mandatory. The one-body fixed density matrix then becomes

$$D(r; r^0) = \int_0^Z dR_1 dR_2 dR_3 (R_1; R_2; R_3 = r) \hat{S}_G^Y \hat{S}_G^0 (R_1; R_2; R_3^0 = r^0); \quad (17)$$

where  $\hat{S}_G$  is the four-body intrinsic nuclear wave function normalized to unity and expressed in terms of the following Jacobi coordinates

$$\begin{aligned} R_1 &= r_2 - r_1; \\ R_2 &= r_3 - (r_2 + r_1) = 2; \\ R_3 &= r_4 - (r_3 + r_2 + r_1) = 3; \end{aligned} \quad (18)$$

The operator  $\hat{S}_G$  given by Eq. (7) is now explicitly written as

$$\hat{S}_G = \prod_{i=1}^3 G(4i); \quad G(4i) = 1 - (z_4 - z_i)(b_4 - b_i); \quad (19)$$

where the longitudinal component  $z_4$  is along the direction of the momentum transfer, which is chosen to coincide with the  $z$ -axis, thus  $r_4$  is expressed as  $r_4 = b_4 + z_4 \hat{q}$ . The standard parametrization for the profile function viz.

$$(b) = \frac{\text{tot} (1 - i)}{4 b_0^2} e^{-b^2/2b_0^2} \quad (20)$$

will be adopted, where  $\text{tot}$  is the total proton-nucleon cross section, and the ratio of the real to the imaginary parts of the forward elastic pN scattering amplitude. In the calculations the values  $i = 0.33$ ,  $b_0 = 0.5 \text{ fm}$  and  $\text{tot} = 43 \text{ mb}$  have been used, which correspond to a kinetic energy of the hit proton  $T_p = 1 \text{ GeV}$ .

The distorted momentum distribution  $n_D(k_m)$  and the nuclear transparency  $T$  are calculated from Eqs. (12) and (15) respectively with  $D$  of Eq. (17).

### III. THE REALISTIC FOUR-BODY WAVE FUNCTION

The  $^4\text{He}$  wave function used in our calculations has been obtained by the variational ATM S method [9,10], according to which

$$\text{ATM S} = F; \quad (21)$$

where  $F$  represents a proper correlation function, and  $S$  is an arbitrary uncorrelated wave function. The correlation function  $F$  has the following form

$$F = D^{-1} \sum_{ij}^X (w(ij) - \frac{(n_p - 1)}{n_p} u(ij)) \sum_{kl \neq ij}^Y u(kl); \quad (22a)$$

$$D = \sum_{ij}^X (1 - \frac{(n_p - 1)}{n_p} u(ij)) \sum_{kl \neq ij}^Y u(kl); \quad (22b)$$

where  $n_p = A(A - 1)/2$  is the number of pairs, and  $w(ij)$  ( $u(ij)$ ) are on-shell (off-shell) two-body correlation functions, respectively. The wave function  $S$  is assumed to be

$$S = fS = 0; T = 0g; \quad (23)$$

where  $f0;0g_A$  represents the antisymmetric spin-isospin function [12] with  $S = T = 0$ , while  $S$  is the fully symmetric spatial function.

The realistic NN interaction generates a state dependence of NN correlations, which is taken into account by introducing the following state dependence for the on-shell correlation function

$$w(ij) = {}^1 w_S(ij) \hat{P}^{1E}(ij) + {}^3 w_S(ij) \hat{P}^{3E}(ij) + {}^3 w_D(ij) \hat{S}_{ij} \hat{P}^{3E}(ij); \quad (24)$$

where  $\hat{P}^{1E}$  ( $\hat{P}^{3E}$ ) is a projection operator to the singlet-even (triplet-even) state and  $\hat{S}_{ij}$  is the usual tensor operator. Tensor-type on-shell correlations are also included in  $F$  (the explicit form of  $F_{ATM S}$  is given in [11]). The best set of correlation functions  $f_{ATM S} = f_{w^0, u^0, sg}$  appearing in Eq. (21) are determined by the Euler-Lagrange equation

$$[ \langle {}_{ATM S} \hat{H} | j_{ATM S} \rangle - E \langle {}_{ATM S} j_{ATM S} \rangle ] = 0; \quad (25)$$

where the variation is performed with respect to each correlation function  $u$ . If a pair product form is assumed for  $w$

$$w = \sum_{ij} (ij); \quad (26)$$

then the radial shape of the two-body function  $f_{ATM S}(ij) = u(ij)(ij)$  can be determined directly from Eq. (25). Thus the ATM S wave function does not contain any free parameter. In the rest of the paper, we use for the realistic NN interaction, the Reid soft core V8 model potential [13]. The calculated binding energy corresponding to the ATM S wave functions is  $E_4 = 21.2$  MeV, the rms radius is  $\langle r^2 \rangle^{1/2} = 1.57$  fm, and the probabilities of the various waves are  $P_S = 87.94\%$ ,  $P_{S^0} = 0.24\%$  and  $P_D = 11.82\%$ .

#### IV. RESULTS OF THE CALCULATIONS: THE NUCLEAR TRANSPARENCY

In this section the results of the calculations of the nuclear transparency will be presented.

Let us first discuss the much debated topic concerning the effects of NN correlations on the transparency. To this end, as a  $w$  of Eq. (26) we introduce a mean-field wave function  $w_0$  defined by an harmonic oscillator state with the correct tail [14], viz.

$$w_0 = \sum_{ij} (r_{ij}); \quad (27a)$$

$$(r) = N \begin{cases} e^{-r^2/8R_0^2} & r < r_0 \\ N^{0e^{-r^2/3}} & r > r_0; \end{cases} \quad (27b)$$

where the quantities  $r_0$  and  $N^0$  are determined by the continuity condition, and  $N$  and  $R_0$  are fixed so as to reproduce, respectively, the asymptotic behaviour of the realistic two-body function  $f_{ATM S}(r)$  and the root mean square radius (1.57 fm) provided by the realistic wave function, i.e.  $N = 0.76$  and  $R_0 = 1.22$  fm. Thus, by calculating the nuclear transparency using the full realistic,  $F_{ATM S}$ , and the mean-field,  $w_0$ , wave functions, one can ascribe any difference in the results to the effect of the correlations.

The results of the calculation are presented in Table I, where it can be seen that the effect of correlations on the transparency, given by the difference between  $T_{ATM S}$  and  $T_0$ , is very small (~3%). We have also calculated  $T$  with the Jastrow-type wave function

$$J = \sum_{ij} f_J(r_{ij}) \quad 0; \quad f_J(r_{ij}) = 1 - e^{-r_{ij}^2/2r_c^2}; \quad (28)$$

used in [6] with  $r_c = 0.5$  fm. It can be seen from Table I that in such a case correlation effects amount to 7%, which is about a factor of two larger than in the realistic case. Since the Jastrow-type correlation function in Eq. (28) takes only into account short-range repulsive correlations, the difference between the realistic and the Jastrow cases should be ascribed to the intermediate-range attractive correlation which is provided by realistic correlation function. In order to clearly illustrate this point, the realistic correlation function  ${}^3w_s(r) = {}^3w_s(r) - (5/6)u(r)$  is compared with the Jastrow one in Fig. 1, and the strong overshooting in the function, which is induced by the attractive correlation, and which is lacking in the Jastrow phenomenological wave function, can be noticed. The attractive correlation enhances FSI effects and, as a result, the nuclear transparency is reduced because of the cancellation between short-range repulsive and intermediate-range attractive correlations.

The tensor-type correlations, which are induced by the realistic interaction, produce a D-wave component in the  ${}^4He$  wave function. The value of the nuclear transparency calculated without the D-wave component, denoted  $T_s$  in table I, does not appreciably differ from the full results ( $T_{ATM}$ ). However, one should not share the mistaken belief that tensor correlations are unimportant, because the shape of the correlation function shown in Fig. 1, which determines the relative strength between repulsive and attractive correlations, is strongly affected by the tensor force through the S-D wave coupling. Therefore, the inclusion of tensor correlations is essential in determining the exact correlation function with the proper overshooting, even if the presence of the D-wave in the wave functions provides only a small contribution to the transparency.

Using an approximate scheme based on central correlations, it has been argued [1] that the effect of correlations on the transparency should be very small because of an almost entire cancellation between the hole and spectator effects. In order to check whether such a conclusion holds in a realistic approach to correlations, we have calculated the hole contribution to the transparency, by removing correlations among all the spectator pairs setting  $f_{ATM}(ij) = 0$  for all spectator-(ij) pairs. The result, denoted by  $T_{ATM}$  (no spect.) in table I, practically does not differ from the full result  $T_{ATM}$ , which includes hole and spectator correlations. This clearly shows that the spectator effect is extremely small and that there is no significant cancellation between hole and spectator correlations.

Let us now discuss the convergence of the Glauber multiple scattering series. To this end, using Eq. (19), the operator  $\hat{S}_G^Y \hat{S}_G^Y$  in Eq. (17) is expanded in the following way

$$\hat{S}_G^Y \hat{S}_G^Y = \sum_X 1 + G_1 + G_2 + G_3; \quad (29a)$$

$$G_1 = \sum_{ij} (G(4ij) - 1);$$

$$G_2 = \sum_{\substack{ij \\ i < j < 4}} (G(4ij) - 1)(G(4j) - 1); \quad (29b)$$

$$G_3 = \sum_{\substack{ij \\ i < 4}} (G(4ij) - 1);$$

Several approaches in the field [3], [4] rely on the truncation of the Glauber multiple scattering series taking into account only the single rescattering term  $G_1$ . In table II

the contribution to the transparency from the various terms of the series in Eq. (29) are presented. It can be seen that  $G_2$  amounts to 14% of the first order contribution  $G_1$ , and its inclusion changes the total  $T$  by about 5%. Therefore the double rescattering term  $G_2$  should not be disregarded in the calculation of the transparency.

## V. RESULTS OF THE CALCULATIONS: THE DISTORTED MOMENTUM DISTRIBUTIONS

In this section the results of the calculations of the distorted momentum distributions will be presented. We will compare our results with the ones obtained in [6] using phenomenological Jastrow wave functions adopting the same form and parameters for  $\rho$  in Eq. (28), namely the harmonic oscillator wave function  $\rho_0$  with parameter  $R_0 = 1.29\text{fm}^{-1}$ , and the central correlation function with parameter  $r_c = 0.5\text{fm}^{-1}$ . We will consider the parallel ( $\theta = 0^\circ; k_\theta = 0$ ), antiparallel ( $\theta = 180^\circ; k_\theta = 0$ ), and perpendicular ( $\theta = 90^\circ; k_\theta = 0$ ) momentum distributions, where  $\theta$  is the angle between the three-momentum transfer  $q$  and  $k_m = q - k_p$ . From now on, the notation  $k \equiv k_m$  will be used. In absence of FSI the three distributions will coincide with the usual momentum distribution  $n(k)$ . The realistic momentum distributions  $n(k)$  corresponding to the ATM S method are shown in Fig. 2, where they are compared with the momentum distributions corresponding to the Jastrow wave function. The numerical integration of  $n(k)$  with realistic wave functions has been performed by the quasi random number (QRN) method [15].

Let us consider the distorted momentum distributions and let us demonstrate that the relevance of FSI effects strongly depends upon the type of ground state wave functions. To this end, we consider the mean field result given by the harmonic oscillator model wave function and the realistic one calculated by the ATM S wave function. The results for the parallel distorted momentum distributions are shown in Fig. 3. It can be seen that:

1. as expected, the main effect of FSI is to enhance the content of high momentum components (cf. Fig. 3(a));
2. FSI are strongly reduced when the correct high momentum content of realistic ground state wave functions is taken into account (cf. Fig. 3(b)).

Let us now compare the effects of FSI in the realistic and Jastrow cases. To this end, the undistorted and distorted (anti)parallel and perpendicular momentum distributions are compared in Fig. 4. The results there shown, clearly exhibit again a strong dependence of FSI upon the type of ground state correlations; it can in particular be seen that FSI are much larger in the Jastrow case. Only in the case of perpendicular kinematics, the distorted momentum distributions appear to be the same in the Jastrow and realistic cases: at  $\theta = 90^\circ$ , Gaussian multiple scattering FSI produces the largest content of high momentum components. Eventually, in Fig. 5 the overall comparison between the realistic and the Jastrow distorted momentum distributions is presented and the following points are worth being noticed:

1. a sizeable difference between Jastrow and realistic wave functions shows up in the low momentum region; such a difference should be ascribed both to the tail behaviour of

the wave functions, with the Jastrow function having the wrong asymptotics, and to the attractive correlation effect discussed in the previous Section.

2. the longitudinal momentum distributions appreciably differ in the high momentum region  $k \gtrsim 2.0 \text{ fm}^{-1}$ , which is mainly due to the effect of the D-wave, which is absent in the Jastrow wave function. The effect of the D-wave component will be discussed below in more details.

In order to better visualize the effect of FSI, the quantity  $R(k) = n_D(k)/n(k)$ , i.e. the ratio between the distorted and undistorted momentum distributions, is presented in Fig. 6. It can be seen that while the parallel and antiparallel ratios are of the order of unity, the perpendicular ratio may reach (in the Jastrow case) almost an order of magnitude. This is a natural result which comes from the Glauber profile function in Eq. (20); in fact, due to its short-range nature in the  $b$  plane, it creates a high momentum components at transverse directions. Thus at perpendicular kinematics, FSI dominates the high momentum component induced by ground state correlations, as pointed out in ref. [6]. However, from a quantitative point of view, its magnitude largely depends upon the nature of correlations, as clearly illustrated by the differences exhibited in Fig. 6 by Jastrow and realistic wave functions. The smaller effect of FSI in the realistic case is mainly due to the D-wave component produced by the tensor-type correlations. As a matter of fact, the D-wave component, being more peripheral with respect to the S-wave component, is less affected by FSI, since for a peripheral nucleon the probability of a collision is reduced. This is clearly demonstrated in Fig. 7 where the angular dependence of the distorted momentum distribution is plotted for a fixed value of the missing momentum  $k$ . The figure shows indeed that the D-wave component (dot-dashed curve) is little affected by FSI (remember that the undistorted momentum distribution is angle independent). In this respect, an interesting quantity is the forward-backward asymmetry  $A_{FB}$  defined as [6]

$$A_{FB}(k) = \frac{n_D(k: \theta = 0) - n_D(k: \theta = 180)}{n_D(k: \theta = 0) + n_D(k: \theta = 180)}: \quad (30)$$

The interest in this quantity, which differs from zero because of the FSI, stems from the following reason: since, as previously illustrated in Fig. 7, the D-wave component has little asymmetry,  $A_{FB}$  gets contribution almost entirely from the S-wave. This suggests that this quantity might give an useful information on the S-wave component. To demonstrate such a point, we have calculated  $A_{FB}$  with the realistic wave function by changing the D-wave probability  $P_D$  within a reasonable range [16]. The results are presented in Fig. 8, which indeed shows that  $A_{FB}$  slightly depend upon the D-wave probability. In the figure the predictions by the Jastrow wave function are also presented and, again, it can be seen that simple phenomenological central correlations produce unreliable results at high missing momenta.

## VI. SUMMARY AND CONCLUSIONS

In this paper we have thoroughly investigated the effects of correlations on the nuclear transparency and distorted momentum distributions of  ${}^4\text{He}$  in the semi-inclusive process

$^4\text{He}(e; e^0 p)X$  within the Glauber approach using a four-body wave function corresponding to a realistic nucleon-nucleon interactions and therefore featuring central and non-central correlations. Our main results can be summarized as follows:

1. The effect of realistic NN correlations on nuclear transparency  $T$  amounts to 3%. Such a small value mainly results from the cancellation between short-range repulsive correlations and intermediate-range attractive correlations originating from the central-tensor coupling, and not from the cancellation between the hole and the spectator correlation contributions, for the latter is always much smaller than the former and thus there is no significant cancellation between them (the same appears to hold for complex nuclei as well [17], [18], [19]). The contribution from double rescattering term, e.g. the ternary collision term  $\beta$  amounts to 14% of the leading order term, the single rescattering contribution. It is clear therefore that the double rescattering contribution should be taken into account even at high momentum transfer region, such as  $Q^2 \approx \text{several (GeV/c)}^2$ , which is the kinematical region considered in this paper.
2. The effect of correlations and Glauber FSI on the distorted momentum distributions significantly depends upon the type of wave functions which are adopted to describe the ground state; if ground-state correlations are completely absent, a situation which does not occur in nature and real nuclei are strongly correlated systems, the whole high momentum content of the distorted momentum distributions is provided by FSI. However its effect is strongly reduced if realistic wave functions embodying ground state correlations are used. Realistic central plus non-central correlations have different effects on the distorted momentum distributions than the ones produced by central Jastrow correlations.
3. The effect of FSI dominates the high momentum component of the perpendicular distorted momentum distributions  $n_D(k_\perp; k_\parallel = 0)$ , though its magnitude is reduced if tensor-type correlations which induce the D-wave component in  $^4\text{He}$  are taken into account.
4. The parallel (antiparallel) distorted momentum distributions  $n_D(k_\perp = 0; k_\parallel)$  are strongly affected at medium and high momenta by the effect of FSI if simple unrealistic uncorrelated or Jastrow centrally correlated wave functions are adopted to describe the  $^4\text{He}$  ground state; if however the latter is described by "real" four-body wave functions, featuring the correct high momentum content in the ground state, the effect of FSI on the high momentum part of  $n_D(k_\perp = 0; k_\parallel)$  is strongly reduced, resulting in a small correction term; thus the longitudinal distorted momentum distributions are a proper quantity to investigate ground state nuclear wave functions without large uncertainties due to FSI effects.
5. The forward-backward asymmetry  $A_{FB}(k)$  represents an interesting quantity to filter out the S-wave component of the four-body wave function.

To sum up, the effect of correlations and Glauber FSI on the nuclear transparency  $T$  and the distorted momentum distributions  $n_D(k)$  significantly depends upon the type of wave

functions which are adopted to describe the  $^4\text{He}$  ground state; the description of the latter in terms of phenomenological Jastrow wave functions embodying only central correlations is not a sufficiently correct starting point.

Calculations for complex nuclei, using a new recently proposed approach to introduce realistic correlations in the treatment of Glauber FSI effects, based on a linked cluster expansion [17] are in progress and will be published elsewhere [18], [19].

#### A C K N O W L E D G M E N T S

This work is in part supported by the Grant of Sapporo Gakuin University. H.M. thanks INFN, Sezione di Perugia, for the hospitality.

## REFERENCES

- [1] N.N. Nikolaev, A. Szczurek, J. Ambach, B.G. Zakharov and V.R. Zoller, *Phys. Lett. B* 317, 281 (1993).
- [2] O. Benhar, A. Fabrocini, S. Fantoni, V.R. Pandharipande and I. Sick, *Phys. Rev. Lett.* 69, 881 (1992).
- [3] A.S. Ratnat and B.K. Jennings, *Nucl. Phys. A* 597, 636 (1996).
- [4] A. Kohama, K. Yazaki and R. Seki, *Nucl. Phys. A* 551, 687 (1993).
- [5] R. Seki, T.D. Shopa, A. Kohama and K. Yazaki, *Phys. Lett. B* 383, 133 (1996).
- [6] A. Bianconi, S. Jeshonnek, N.N. Nikolaev and B.G. Zakharov, *Phys. Lett. B* 338, 123 (1994); *B* 363, 217 (1995).
- [7] A. Bianconi, S. Jeshonnek, N.N. Nikolaev and B.G. Zakharov, *Phys. Lett. B* 343, 13 (1995).
- [8] L.L. Frankfurt, M. Sargsyan and M.I. Strikman, *Phys. Rev. C* 56, 1024 (1997).
- [9] M. Sakai, I. Shimodaya, Y. Akashi, J. Hiiura and H. Tanaka, *Prog. Theor. Phys. Suppl.* No. 56, 32 (1974).
- [10] Y. Akashi, *Cluster Model and Other Topics (World Scientific)*, p. 335 (1987).
- [11] H. Morita, Y. Akashi, O. Endo and H. Tanaka, *Prog. Theor. Phys.* 78, 1117 (1987).
- [12] J.E. Beam, *Phys. Rev.* 158, 907 (1967).
- [13] I.E. Lagaris and V.R. Pandharipande, *Nucl. Phys. A* 359, 331 (1981);
- [14] I.R. Afnan and Y.C. Tang, *Phys. Rev.* 175, 1337 (1968).
- [15] H. Tanaka and H. Nagata, *Progr. Theor. Phys. Suppl.* 56, 121 (1974).
- [16] S. Rosati, M. Viviani and A. Kievsky, in *Few-Body Problems in Physics '95*, *Few Body Systems*, Suppl. 8, 21 (1995).
- [17] C. Ciodegli Atti and D. Treleani, to be published.
- [18] C. Ciodegli Atti, H. Morita and D. Treleani, talk given at the Elba Workshop on Electron Scattering from Nuclei, EIPC, June 1998, to appear in the Proceedings. nucl-th/9811102.
- [19] C. Ciodegli Atti, H. Morita and D. Treleani, in preparation.

TABLES

TABLE I. The results of the nuclear transparency  $T$ .

$T_0$	$T_{ATM\ S}$	$T_{Jastrow}$	$T_S$	$T_{ATM\ S}$ (no spect.)
0.754	0.778	0.806	0.780	0.778

TABLE II. Higher order contribution of Glauber multiple scattering series to the nuclear transparency  $T$ .

	$G_1$	$G_2$	$G_3$	Total
1	-0.2566	0.0363	-0.0021	0.778

## FIGURES

FIG. 1. The realistic correlation function in the triplet S state  ${}^3w_s(r) = {}^3w_s(r) - (5/6)u(r)$  appearing in Eq. (24) (full) compared with the Jastrow-type correlation function  $f_J(r)$  defined by Eq. (28) (dashed).

FIG. 2. The realistic momentum distribution (full) compared with the momentum distribution obtained with the phenomenological Jastrow wave function (dashed).

FIG. 3. The parallel momentum distributions ( $\theta = 0$ ) corresponding to the harmonic oscillator model wave function (a) and to the realistic correlated variational wave function (Eq. (21)) (b). The dashed curves represent the undistorted (No FSI) momentum distributions, whereas the full curves include FSI.

FIG. 4. Comparison of the parallel ( $\theta = 0$ ), antiparallel ( $\theta = 180$ ), and perpendicular ( $\theta = 90$ ) distorted momentum distributions calculated using realistic (Realistic) (a) and (b)) and Jastrow (Jastrow) (c) and (d)) ground state wave functions including (FSI) and omitting (No FSI) final state interactions.

FIG. 5. The overall comparison between the distorted momentum distributions calculated using realistic (full) and Jastrow (dashed) ground state wave functions. Here (a)–(c) corresponds to the parallel ( $\theta = 0$ ), perpendicular ( $\theta = 90$ ) and antiparallel ( $\theta = 180$ ) kinematics respectively.

FIG. 6. The ratio between the distorted and undistorted momentum distributions  $R(k) = n_D(k)/n(k)$  corresponding to the realistic (Realistic) and Jastrow (Jastrow) ground state wave functions (note the different vertical scales).

FIG. 7. The angular dependence of the distorted momentum distributions  $n_D(k)$  at fixed value of the missing momentum  $k_m$  ( $k = 3.0 \text{ fm}^{-1}$ ). The various curves show the contributions from the different  ${}^4\text{He}$  waves. The practically constant value of the D wave contribution demonstrates that FSI mostly act on the S wave.

FIG. 8. The forward-backward asymmetry  $A_{FB}(k)$  defined by Eq. (30) calculated with realistic (full) and Jastrow (dashed) wave functions. The dot-dashed and short-dashed curves correspond to the realistic wave function with modified D-wave probability, namely  $P_D = 10.0\%$  and  $15.0\%$  respectively.

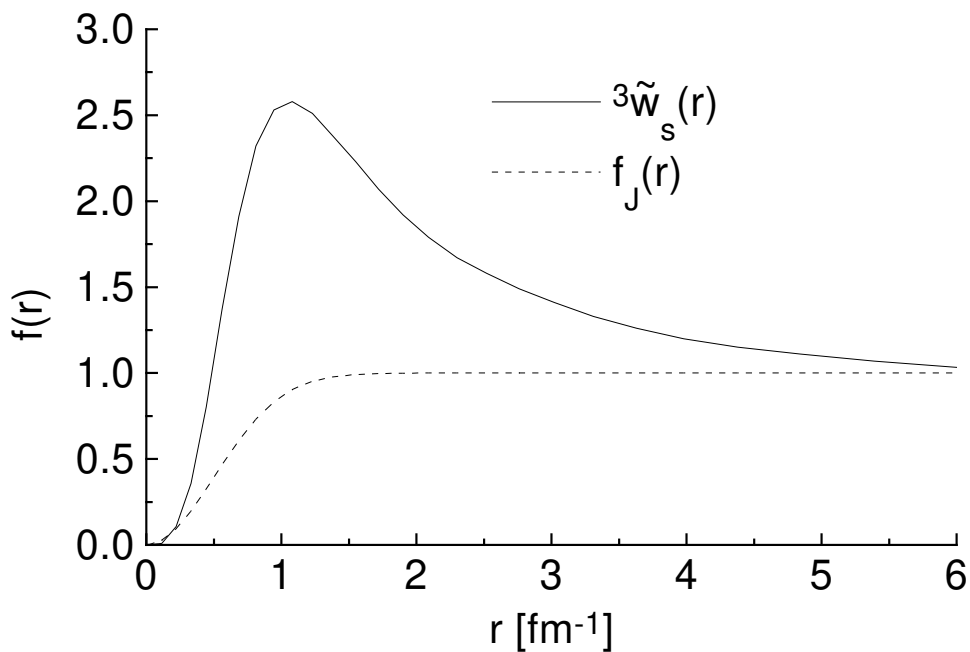


Fig. 1

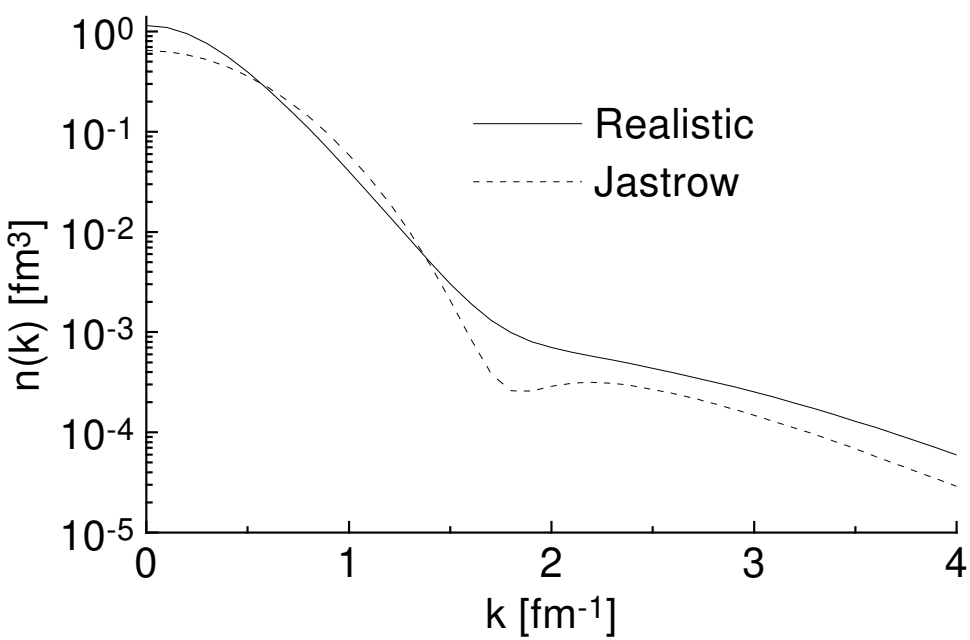


Fig. 2

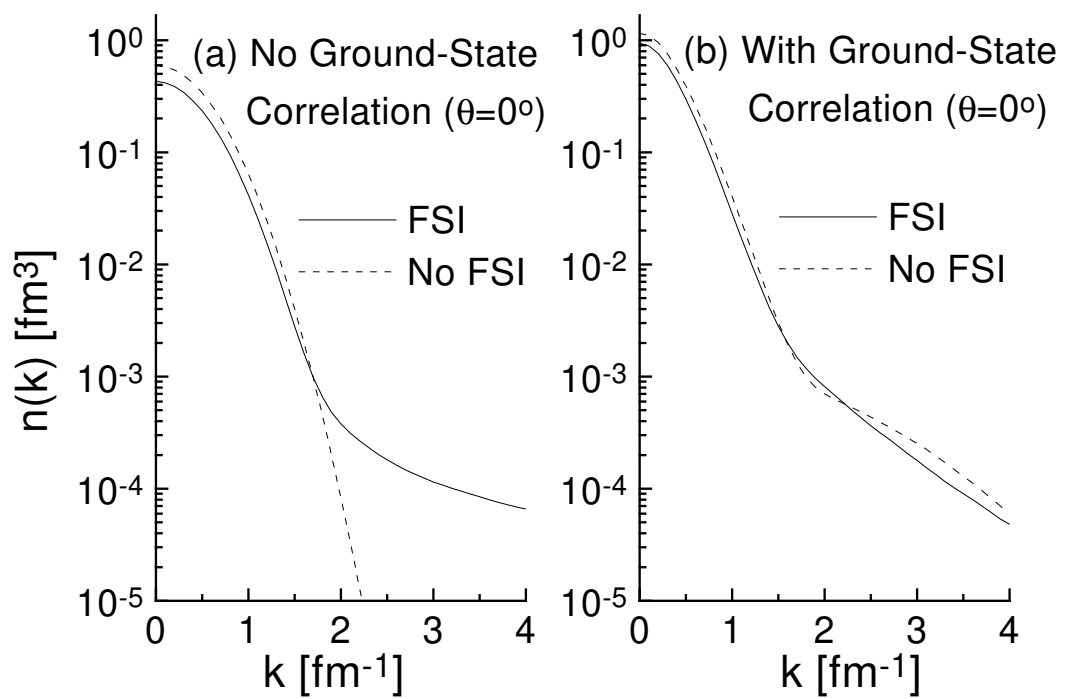


Fig.3

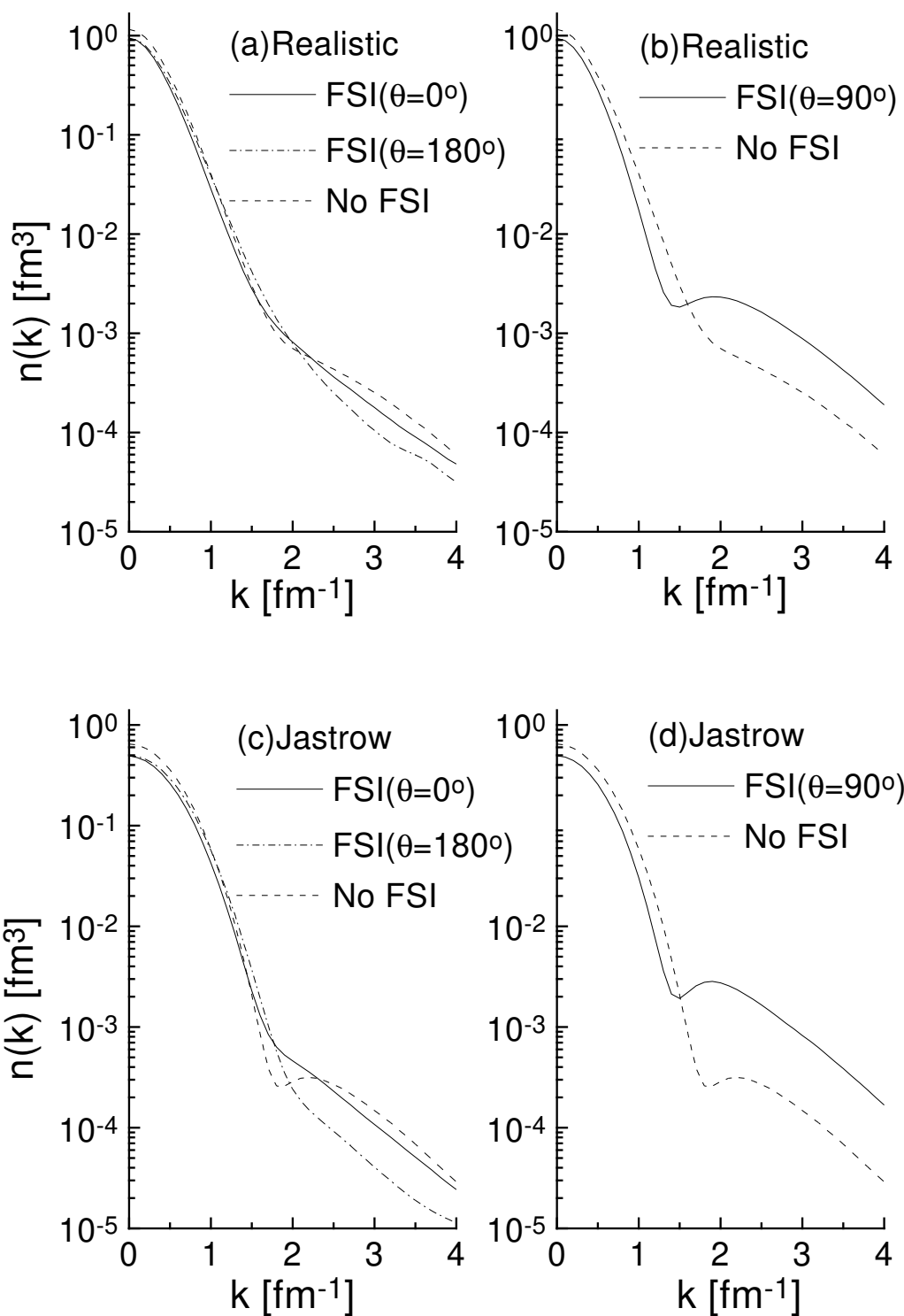


Fig. 4

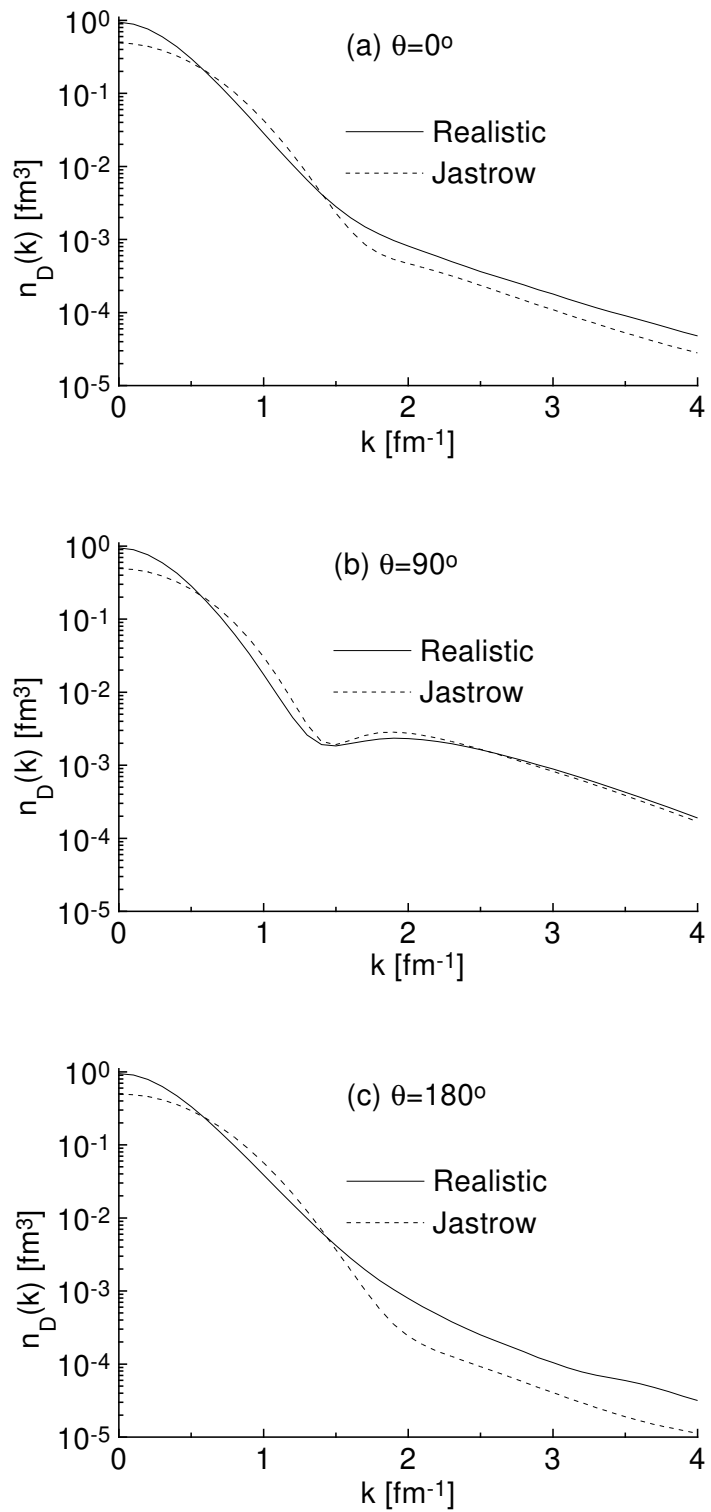


Fig. 5

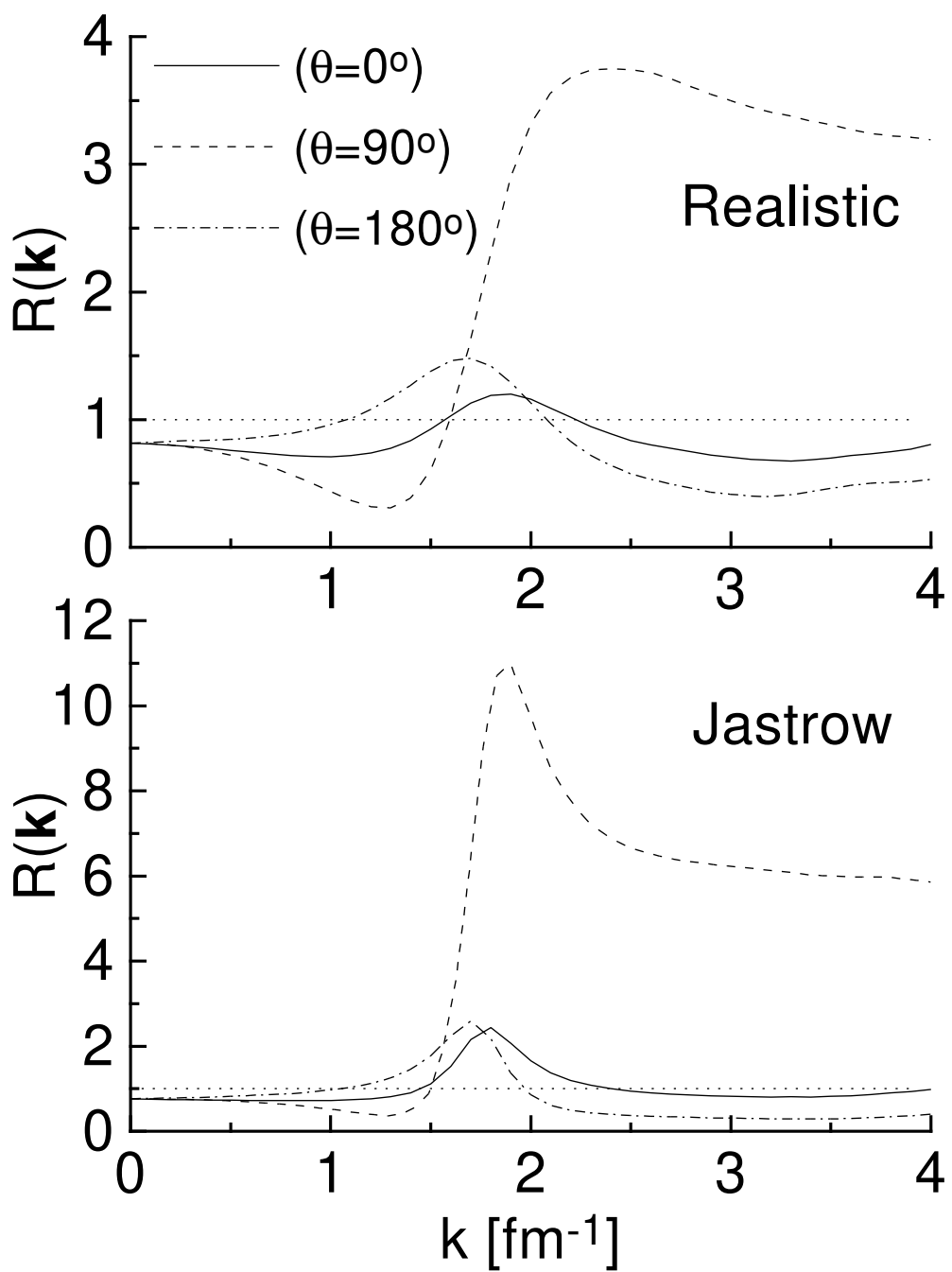


Fig. 6

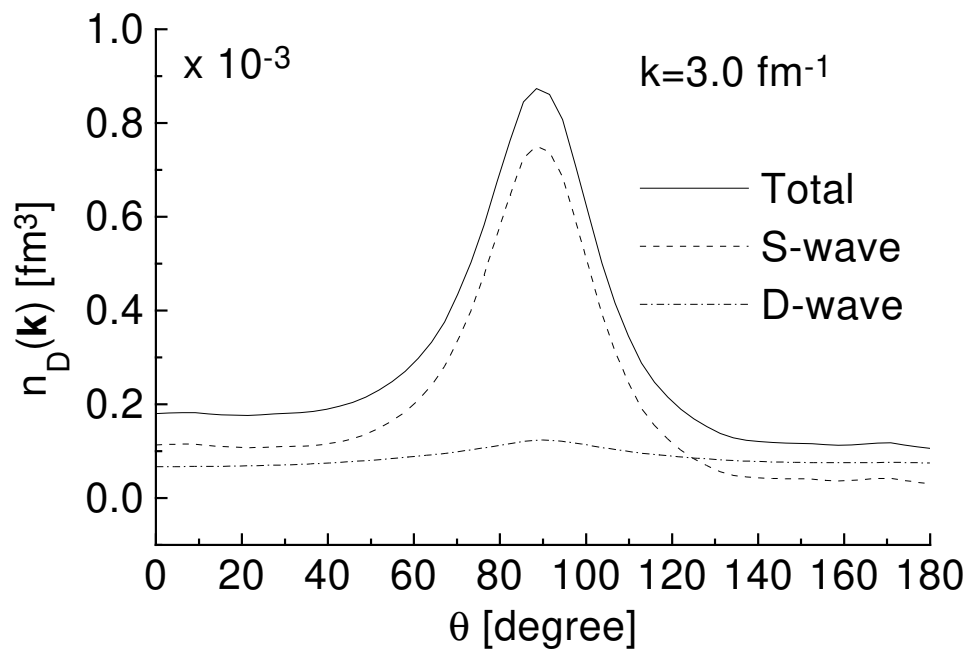


Fig. 7

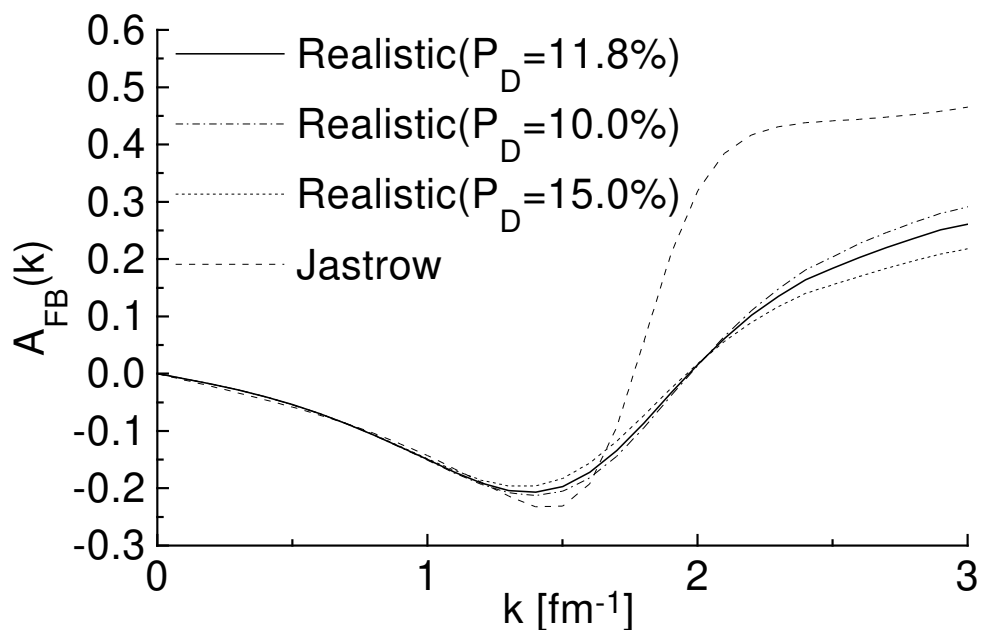


Fig. 8